AMERICAN SOCIETY FOR MICROBIOLOGY | Journal of Bacteriology

Regulation of a Protein Acetyltransferase in *Myxococcus xanthus* by the Coenzyme $NADP^+$

Xin-Xin Liu, Wei-bing Liu, Bang-Ce Ye

Lab of Biosystems and Microanalysis, State Key Laboratory of Bioreactor Engineering, East China University of Science and Technology, Shanghai, China

ABSTRACT

$NADP^+$ is a vital cofactor involved in a wide variety of activities, such as redox potential and cell death. Here, we show that $NADP^+$ negatively regulates an acetyltransferase from *Myxococcus xanthus*, Mxan_3215 (*Mx*Kat), at physiologic concentrations. *Mx*Kat possesses an NAD(P)-binding domain fused to the Gcn5-type *N*-acetyltransferase (GNAT) domain. We used isothermal titration calorimetry (ITC) and a coupled enzyme assay to show that $NADP^+$ bound to *Mx*Kat and that the binding had strong effects on enzyme activity. The Gly11 residue of *Mx*Kat was confirmed to play an important role in $NADP^+$ binding using site-directed mutagenesis and circular dichroism spectrometry. In addition, using mass spectrometry, site-directed mutagenesis, and a coupling enzymatic assay, we demonstrated that *Mx*Kat acetylates acetyl coenzyme A (acetyl-CoA) synthetase (Mxan_2570) at Lys622 in response to changes in $NADP^+$ concentration. Collectively, our results uncovered a mechanism of protein acetyltransferase regulation by the coenzyme $NADP^+$ at physiological concentrations, suggesting a novel signaling pathway for the regulation of cellular protein acetylation.

IMPORTANCE

Microorganisms have developed various protein posttranslational modifications (PTMs), which enable cells to respond quickly to changes in the intracellular and extracellular milieus. This work provides the first biochemical characterization of a protein acetyltransferase (*Mx*Kat) that contains a fusion between a GNAT domain and $NADP^+$-binding domain with Rossmann folds, and it demonstrates a novel signaling pathway for regulating cellular protein acetylation in *M. xanthus*. We found that $NADP^+$ specifically binds to the Rossmann fold of *Mx*Kat and negatively regulates its acetyltransferase activity. This finding provides novel insight for connecting cellular metabolic status ($NADP^+$ metabolism) with levels of protein acetylation, and it extends our understanding of the regulatory mechanisms underlying PTMs.

The dynamic and reversible mechanism of protein acetylation is an important regulatory posttranslational modification (PTM), which controls numerous cellular processes in the three kingdoms of life (1–4). Recent studies have identified >4,500 acetylated proteins, ranging from transcription factors and ribosomal proteins to many metabolic enzymes that are related to glycolysis, gluconeogenesis, the tricarboxylic acid (TCA) cycle, and fatty acid, nitrogen, and carbon metabolism (3, 5–8). Following the discovery of acetylation of the *Salmonella enterica* acetyl coenzyme A (acetyl-CoA) synthetase in 2002 (9), this type of PTM has also emerged as an important metabolic regulatory mechanism in bacteria. In the last decade, lysine acetylation of proteins has also been reported in other organisms (6, 7, 10–16).

Protein lysine acetylation can occur via either enzymatic or nonenzymatic acetylation, such as chemical acetylation. Intracellular acetyl phosphate (AcP) plays a critical role in a chemical acetylation reaction; for example, AcP has been shown to chemically acetylate histones, serum albumin, and synthetic polylysine *in vitro* (17). In addition, recent research has shown that AcP can chemically acetylate lysine residues, and acetate metabolism can globally affect the level of protein acetylation in *Escherichia coli*. In addition, mutant cells that did not synthesize AcP or convert AcP to acetate, leading to its accumulation, showed significantly reduced or elevated acetylation levels *in vivo*, respectively (5). This finding suggests that the intracellular AcP concentration is correlated with protein acetylation levels (5, 7, 8).

The proportion of enzymatic acetylation reactions in the cell is relatively small compared to that of chemical acetylation reactions (7), and enzymatic acetylation in bacteria requires protein acetyltransferases and deacetylases. Protein acetyltransferases control the acetylation of specific proteins under various physiological conditions, whereas protein deacetylases play a role in removing the acetyl group from some acetylated proteins in response to changes in the cellular energy status via promptly sensing the intracellular NAD (NAD^+)-to-NADH ratio (5, 7, 18). In addition to deacetylating the proteins acetylated by acetyltransferases, protein deacetylases also specifically deacetylate the lysines acetylated by AcP (18).

Gcn5-type *N*-acetyltransferase (GNAT) acetyltransferases catalyze the transfer of the acetyl group from the acetyl-CoA donor to a primary amine of small molecules and proteins that are involved in a wide variety of cellular processes. GNATs, named for the

Received 8 August 2015 **Accepted** 18 November 2015

Accepted manuscript posted online 23 November 2015

Citation Liu X-X, Liu W-B, Ye B-C. 2016. Regulation of a protein acetyltransferase in *Myxococcus xanthus* by the coenzyme $NADP^+$. J Bacteriol 198:623–632. doi:10.1128/JB.00661-15.

Editor: W. W. Metcalf

Address correspondence to Wei-bing Liu, lwb@ecust.edu.cn, or Bang-Ce Ye, bcye@ecust.edu.cn.

Supplemental material for this article may be found at http://dx.doi.org/10.1128/JB.00661-15.

homology to the yeast GCN5 protein (yGCN5p), are characterized by signature sequence motifs and structural homology (19). GNATs are conserved in all domains of life and represent one of the largest protein superfamilies (20). GNATs are involved in the acetylation of antibiotics, hormones, tRNA, histones, metabolic enzymes, and transcription factors and are thus implicated in a wide variety of cellular processes (4, 20–23).

Transcriptional and posttranslational regulation mechanisms of GNAT protein acetyltransferases have been demonstrated. For instance, regulation of the expression of the *acuA* gene, which encodes an acetyltransferase in *Bacillus subtilis*, is under the control of CcpA, a global regulatory protein that is affected by the quality of the carbon source available to the cell (24). In *E. coli*, transcription of the acetyltransferase PatZ (also known as YfiQ or Pka) is controlled at the transcriptional level by intracellular cyclic AMP (cAMP) levels. The catabolite activator protein (CAP)-cAMP complex has been proposed to bind to two sites in the *patZ* promoter to induce the expression of genes that increase the overall acetylation of proteins (25, 26).

The activity of protein acetyltransferases is also allosterically controlled by small biological molecules. Recently, we found that the amino acid-binding (ACT) domain is fused to the GNAT acetyltransferase in *Micromonospora aurantiaca* (*Ma*Kat), which confers amino acid-induced allosteric regulation (11). Similarly, fusion of the cAMP domain to the GNAT domain can occur in response to various stress conditions (i.e., cAMP concentration) to modulate the activity of a GNAT protein acetyltransferase in mycobacteria (27–30). Here, we report a new acetyltransferase found in *M. xanthus* (*Mx*Kat), which is encoded by the gene Mxan_3215 and contains both GNAT- and NAD(P)-binding Rossmann-type fold domains, similar to the cAMP-GNAT and ACT-GNAT domain organizations reported previously (11).

Similar to amino acids and cAMP, the coenzyme $NADP^+$ is a small molecule that plays a very important role in many biological processes. For instance, $NADP^+$ is a required cofactor in the reductive biosynthesis of fatty acids, isoprenoids, and aromatic amino acids (31). Furthermore, the NAD(P) coenzyme may perform very important regulatory functions in various physiologic settings. For example, $NADP^+$ can induce a surrounding signal, such as reactive oxygen species, to regulate function (32). As the reverse reaction product of acetylation, NAD^+ is required for many bacterial NAD^+-dependent deacetylases (33–35). Thus, we hypothesized that $NAD(P)^+$ coenzymes are specific regulatory ligands that may modulate the acetylation activity of *Mx*Kat in *M. xanthus*.

To test the hypothesis, we screened four coenzymes (NAD^+, NADH, $NADP^+$, and NADPH) using Western blot analysis to evaluate their influence on the acetylation activity of *Mx*Kat. Furthermore, isothermal titration calorimetry (ITC) was used to analyze the interaction between each coenzyme and *Mx*Kat. We found that $NADP^+$ specifically bound to *Mx*Kat and was strongly bound under physiologic concentrations. Further, we found that *Mx*Kat is an $NADP^+$ concentration-dependent acetyltransferase. Through a site-directed mutant assay, we characterized the active site of $NADP^+$ binding and acetylation of the acetyl-CoA synthetase *Mx*Acs, a substrate of *Mx*Kat. These data will help elucidate the mechanism by which $NADP^+$ regulates *Mx*Kat to affect the acetylation of specific proteins.

MATERIALS AND METHODS

Cloning, overexpression, and purification of proteins. We amplified the Mxan_3215 and Mxan_2570 genes by PCR from the genomic DNA of *M. xanthus* DK 1622 using two primer pairs (5′-TAAGAATTCATGACGCC TCCTCTCGTCCTCC and TAAAAGCTTTCACAGGGTGAGGACCAT CAACTCC-3′, and 5′-TAAGAATTCTTGTCCACGCTGGAGGAACG and TAAAAGCTTTCAGTCGTCGTTCTGCCTCAGC-3′). After digestion with the restriction enzymes EcoRI and HindIII, we cloned the genes encoding the Mxan_3215 and Mxan_2570 proteins into the pET-28a vector to generate PET28a-Mxan_3215 and PET28a-Mxan_2570, and we sequenced the clones for verification. *E. coli* strain BL21(DE3) was used for protein expression. We selected and cultured a single colony in a 3-ml overnight culture, which was used to inoculate 50 ml of Luria-Bertani medium with 1% kanamycin. The cells were cultivated at 37°C and then induced with 0.7 mM isopropyl-β-D-thiogalactoside at 20°C overnight. Next, we centrifuged the culture to obtain the cells, which were resuspended in phosphate-buffered saline (PBS) buffer (137 mM NaCl, 2.7 mM KCl, 10 mM Na_2HPO_4, 1.8 mM KH_2PO_4 [pH 7.4]) and incubated on ice for 15 min. The cells were sonicated in PBS buffer, and cell debris was removed by centrifugation at 8,000 rpm for 20 min. A nickel-nitrilotriacetic acid (Ni-NTA)–agarose column was used to purify the supernatant, and the bound protein was preequilibrated with the binding buffer. After the flowthrough was discarded, the column was washed with 10 ml of washing buffer (300 mM NaCl, 50 mM NaH_2PO_4, and 20 mM imidazole [pH 8.0]) to eliminate the hybrid proteins, and the bound proteins were eluted with a linear gradient of 20 to 250 mM imidazole in washing buffer. Sodium dodecyl sulfate-polyacrylamide gel electrophoresis (SDS-PAGE) was used to analyze the fractions, and fractions containing the desired protein were pooled and dialyzed against buffer P (37 mM NaCl, 10 mM Na_2HPO_4, 2.7 mM KCl, 1.8 mM KH_2PO_4, 5% glycerol [pH 7.9]). The His tag of Mxan_3215 was removed by digestion with thrombin (at 4°C overnight). The protein was concentrated using an Amicon Ultra-4 30,000-molecular-weight-cutoff centrifugal device (Millipore, Billerica, MA, USA). The bicinchoninic acid (BCA) assay was used to monitor the protein concentration, using buffer P as the control. The amount of protein after concentration was also analyzed by SDS-PAGE.

Analysis of the protein–small-molecule interaction using ITC. ITC is a powerful approach in which the heat released or absorbed throughout a titration reaction is measured. Calorimetric measurements were performed at 25°C with an iTC200 system (MicroCal; GE Healthcare, USA). All solutions were thoroughly degassed before use by stirring them under vacuum conditions. *Mx*Kat protein and $NADP^+$ were dissolved in 1 M PBS (pH 7.4) and then used for ITC to investigate the interaction between *Mx*Kat and $NADP^+$. Calorimetric data were analyzed using Origin for ITC version 7.0383.

Phylogenetic analysis of the NAD(P)-binding domain in *M. xanthus*. The boundaries of the NAD-binding domain in *Mx*Kat were identified by analysis in the Pfam database (http://pfam.xfam.org/). The sequence of the defined domain was used to identify orthologs in the Swiss-Prot database using BLASTp. Individual full-length sequences of the hits obtained were then analyzed using Pfam to identify their NAD-binding domains. Furthermore, the protein sequence analysis of *Mx*Kat using the Conserved Domain Database (CDD) (36) demonstrated that the NAD-binding domain of *Mx*Kat belonged to cd05266 (http://www.ncbi.nlm.nih.gov/Structure/cdd/cddsrv.cgi?uid=187576). All sequences were then aligned using Clustal W (EMBL). The alignments were edited using JalView, and phylogenetic and molecular evolutionary analyses were conducted using Molecular Evolutionary Genetics Analysis (MEGA) software version 6 (37).

Determination of the acetyltransferase activity of *Mx*Kat. To successfully monitor the acetylation reaction activated by *Mx*Kat, a coupling enzyme activity reaction was established. One of the products of the acetylation reaction, CoA, is used by pyruvate dehydrogenase to convert NAD^+ to NADH, which causes an increase in the absorbance at 340 nm (38, 39). The reaction mixture used to assay enzyme activity was opti-

mized using 5 mM $MgCl_2$, 2.4 mM pyruvate, 1 mM dithiothreitol (DTT), 0.2 mM thiamine PP_i (TPP), 0.2 mM NAD, 50 μM acetyl-CoA, 13 μM acetyl-CoA synthetase (Acs), 0.03 U pyruvate dehydrogenase, 0.65 μM *Mx*Kat with or without coenzyme, 100 mM sodium acetate, 50 mM bis-Tris, and 50 mM Tris (pH 7.5) in a total volume of 300 μl. All components except for *Mx*Kat were mixed and incubated at 25°C for 10 min. The reaction was initiated by adding *Mx*Kat, and the reaction speed was determined by monitoring the production of NADH for 10 min. Each measurement was repeated three times.

***In vitro* protein acetylation assays.** To determine whether Mxan_2570 is a substrate of *Mx*Kat, 0.2 μM purified *Mx*Kat protein or bovine serum albumin (BSA) and 5 μM purified unacetylated *Mx*Acs protein were added to a reaction mixture (200 μl total volume) containing 0.05 M HEPES buffer (pH 7.5), 200 μM Tris (2-carboxyethyl) phosphine hydrochloride, and 20 μM acetyl-CoA. The reaction mixtures were incubated at 37°C for 2 h (15). After the reaction, the *Mx*Acs protein samples were divided into two portions: one was analyzed by SDS-PAGE and Western blotting, and the other was used for measurement of Acs activity. The acetylated *Mx*Acs was isolated by SDS-PAGE and then analyzed by liquid chromatography-tandem mass spectrometry (LC-MS/MS).

***In vitro* Acs assays.** *Mx*Acs was incubated with *Mx*Kat, acetyl-CoA (60 μM), and $NADP^+$ (2 μM) at 37°C for 60 min. After the reaction, the acetylated *Mx*Acs was isolated from the reaction mixture by gel filtration and ultrafiltration. The activity of acetylated *Mx*Acs was measured in a coupled enzymatic assay in which CoA was used by malate dehydrogenase to convert NAD^+ to NADH, resulting in an increase in absorbance at 340 nm. The standard reaction mixture contained 100 mM Tris-HCl (pH 7.7), 10 mM L-malate, 0.2 mM CoA, 8 mM ATP (pH 7.5), 1 mM NAD^+, 10 mM $MgCl_2$, 3 units of malate dehydrogenase, 0.4 units of citrate synthase, 100 mM potassium acetate, and various amounts of *Mx*Acs (acetylated and nonacetylated).

Western blotting assays. The sample concentrations were verified using a BCA protein assay kit (Tiangen). Protein samples were then separated by SDS-PAGE and transferred to a polyvinylidene fluoride membrane for 30 to 60 min at 100 V. The membrane was sealed at 24°C in sealing solution, which includes 1× TBST (20 mM Tris-HCl [pH 7.5], 150 mM NaCl, and 0.1% Tween 20) and 5% nonfat dry milk (NFDM), for 120 min. Antiacetyllysine (anti-AcK) antibody was used at a dilution of 1:15,000 in TBST–0.5% NFDM. After incubation at 4°C overnight, the blot was washed three times with TBST. The membrane was incubated with 1 μg/ml horseradish peroxidase-conjugated anti-mouse IgG (in TBST with 3% BSA) at ambient temperature for 120 min. We used an enhanced chemiluminescence system (Pierce, USA) to detect the signal combined with a luminescent image analyzer (DNR Bio-Imaging Systems, Israel), according to the manufacturer's instructions.

Mass spectrometry for analysis of the acetylation site. Protein bands were extracted from the gel and repeatedly washed with 50% ethanol to remove the stain. The gel pieces were dehydrated in acetonitrile and then dried in a centrifugal evaporator (Thermo Fisher Scientific, MA). The gel piece was then treated with 10 mM DTT in 50 mM ammonium bicarbonate and alkylated with 50 mM iodoacetamide in 50 mM ammonium bicarbonate. The pieces were washed with wash solution, dehydrated again, and then rehydrated in 50 mM ammonium bicarbonate with 10 ng/μl trypsin (Promega, Madison, WI); subsequently, digestion continued at 37°C for 12 h. Extraction buffer (75% acetonitrile and 0.1% trifluoroacetic acid) was added to the gel pieces to extract the peptides. The extracts were pooled and concentrated in a centrifugal evaporator.

The sample was dissolved using 4 μl of solvent A (0.1% [vol/vol] formic acid and 2% acetonitrile in water), and the solution was injected into a manually packed reversed-phase column and eluted with a 60-min gradient at a flow rate of 300 nl/min. The high-performance liquid chromatography eluate was directly electrosprayed into an LTQ Orbitrap Elite mass spectrometer (Thermo Fisher Scientific). The mass spectrometric analysis was carried out with an automatic switch between a full MS scan using Fourier transform mass spectroscopy in the Orbitrap device and an MS/MS scan using collision-induced dissociation in the dual linear ion trap. Full MS spectra with an *m/z* range of 350 to 1,700 were acquired with a resolution (full width at half maximum [FWHM]) of 240,000. The five most intense ions in each full MS spectrum were sequentially isolated for MS/MS fragmentation with a normalized collision energy of 35%. Automatic gain control was set at 3E4 for ion trap and at 1E6 for Orbitrap.

Thermo Proteome Discoverer (Thermo Fisher Scientific) was used to generate .mgf files that were subsequently checked against the Mxan_2570 sequence with the Mascot search engine (version 2.3.01; Matrix Science, United Kingdom). The search parameters were enzyme, trypsin; missed cleavage, 2; fixed modification, carbamidomethyl-C; variable modification, acetyl (protein N-term), oxidation-M, and acetylation-K; peptide mass tolerance, 10 ppm; fragment mass tolerance, 0.5 Da; and selected charge states, +2, +3, and + 4.

Site-directed mutagenesis and purification of Mxan_2570 and Mxan_3215. The K622Q mutation was introduced into the recombinant plasmid PET28a-Mxan_2570 using the QuikChange mutagenesis kit (TransGen, Beijing, China). The G9A and G11A mutations in PET28a-Mxan_3215 were introduced in the same way. The mutations were confirmed by DNA sequencing. The expression and purification of the mutant proteins were performed according to the same procedures described above.

Circular dichroism spectrometry assay. Purified wild-type (WT) Mxan_3215 protein and the G11A mutant protein were evaluated using circular dichroism spectrometry (Applied Photophysics, Leatherhead, United Kingdom) in the far-UV region (190 to 260 nm) at room temperature using a 10-mm cuvette. All samples were desalted, and the buffer was exchanged with PBS buffer (pH 7.4) using a Zeba desalt spin column (Thermo Scientific, Pierce, Rockford, IL). The sample solutions were diluted to a concentration of 3 μM. The circular dichroism spectrum scan of every sample was performed in triplicate.

RESULTS

***Mx*Kat showed an NAD(P)-GNAT domain organization and was confirmed to be a protein acetyltransferase.** Previous research demonstrated that proteins containing a GNAT domain can catalyze the acetylation of Acs to modulate its activity (10–12, 40). Furthermore, small molecules can bind to the multidomain acetyltransferase to regulate its activity in response to environmental signals. Here, we focused on the multidomain acetyltransferase Mxan_3215 (*Mx*Kat) derived from *M. xanthus*. Pfam version 27.0 (41) analysis showed that Mxan_3215 contains a GNAT domain and an NAD(P)-binding domain in the C and N termini at residues 273 to 437 and 5 to 185, respectively (Fig. 1A). The amino acid sequence of the GNAT domain in *Mx*Kat was aligned with that of *Ma*Kat (Micau_1670 in *Micromonospora aurantiaca*) (11), *Ms*Pat (MSMEG_5458 in *Mycobacterium smegmatis*) (27), *Mt*-PatA (Rv0998 in *Mycobacterium tuberculosis*) (27), 1Z4RA (human GCN5 acetyltransferase) (42), 1YGHB (yeast histone acetyltransferase) (43), and 1M1DA (tetrahymena GCN5 acetyltransferase) (44) to analyze the possible motif. The results showed a strong similarity between *Mx*Kat and several other types of acetyltransferases; they share the common core motif of the GNAT domain, R/Q-X-X-G-X-G/A (Fig. 1B). This motif was found to be important for acetyl-CoA recognition and binding (45). Using SWISS-MODEL (46) analysis, a three-dimensional model of the GNAT domain of *Mx*Kat was generated (see Fig. S1 in the supplemental material); the conserved pivotal residues, R366 and G369, were predicted to be in the junction of the α-helix and β-sheet, while the G371 residue was predicted to be at the end of the α-helix. In addition, phylogenetic analysis was conducted using MEGA with the GNAT domain sequences of various acetyltransferases, and the results showed that *Mx*Kat clustered with *Ec*PatZ from *E. coli* (25), *Se*Pat from *Sal-*

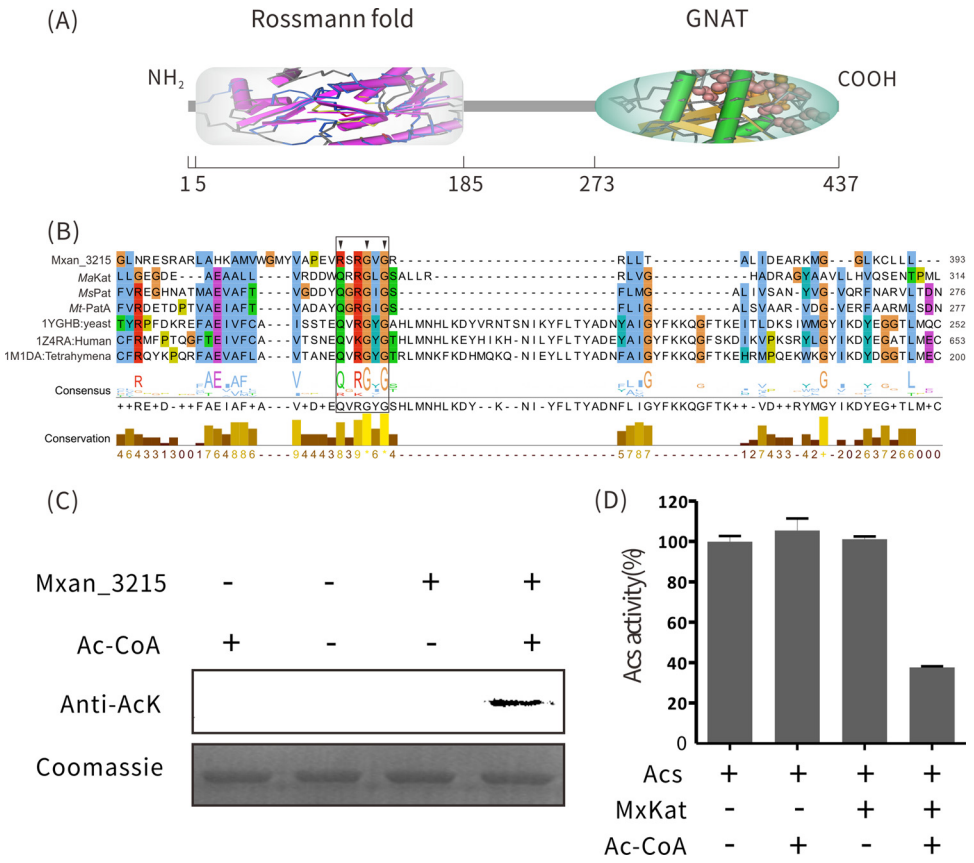

FIG 1 *Mx*Kat is a protein acetyltransferase. (A) Illustration of the domain organization of Mxan_3215. The protein sequence of Mxan_3215 was analyzed in http://pfam.xfam.org/search/sequence, and the result indicated that Mxan_3215 has two domains, one for NAD(P) binding (positions 5 to 185) and one GNAT domain (positions 273 to 437). (B) Multiple sequence alignments of protein acetyltransferases in various species, including *Ma*Kat (*M. aurantiaca*), *Ms*Pat (*M. smegmatis*), Rv0998 (*Mt*-PatA, *M. tuberculosis*), 1YGHB (yeast histone acetyltransferase), 1Z4RA (human GCN5 acetyltransferase), 1M1DA (tetrahymena GCN5 acetyltransferase), and Mxan_3215 (*Mx*Kat, *M. xanthus*). The binding motif is boxed, and key amino acids of the Rossmann fold are marked with arrowheads. (C). Purified *Mx*Acs was incubated with or without *Mx*Kat and acetyl (Ac)-CoA *in vitro* at 37°C for 2 h. After incubation, samples were collected and analyzed by SDS-PAGE, and the acetylation levels were determined by Western blotting using a specific anti-AcK antibody. (D) *In vitro* acetylation affected the activity of *Mx*Acs. *Mx*Acs enzyme activity was measured after incubation with or without acetyl-CoA in the presence of *Mx*Kat for the indicated times. The *Mx*Acs activity is shown as a percentage of the maximum activity determined for *Mx*Acs before acetylation. The data are expressed as the means ± standard deviations (SD) of the results from three identical assays.

monella enterica (47), *Rp*Pat from *Rhodopseudomonas palustris* (16), *Ma*Kat (11), *Mt*-PatA, and *Ms*Pat (48) (see Fig. S2 in the supplemental material). All of these acetyltransferases have been shown to acetylate Acs in different bacteria, which suggests that *Mx*Kat is an acetyltransferase in *M. xanthus* that may also acetylate Acs.

To confirm whether *Mx*Kat, which contains a GNAT domain, actually functions as an acetyltransferase, we incubated purified *Mx*Kat with acetyl-CoA and recombinant *Mx*Acs (Mxan_2570) *in vitro*. The Western blotting results demonstrated that *Mx*Kat has protein lysine acetyltransferase activity for acetylating Acs (Fig. 1C).

To investigate the effect of this acetylation on enzyme activity, *Mx*Acs was incubated with *Mx*Kat in the presence or absence of acetyl-CoA for 2 h. In the presence of both acetyl-CoA and *Mx*Kat, *Mx*Acs activity was reduced, indicating that lysine acetylation effectively decreased *Mx*Acs activity (Fig. 1D).

Characterization of molecular binding with the regulatory NAD(P)-binding domain under physiological conditions. The NAD(P)-binding domain of *Mx*Kat belongs to the cd05266 subfamily of the NAD(P)-binding family. To determine the specific coenzyme molecule that modulates *Mx*Kat activity, we evaluated four coenzymes, NAD, NADH, $NADP^+$, and NADPH, using Western blot analysis. The acetylation was attenuated only when the component contained $NADP^+$, which demonstrated that only $NADP^+$ affected the acetylation function of *Mx*Kat on *Mx*Acs (Fig. 2A). To further determine the binding affinity of $NADP^+$ to *Mx*Kat, we performed ITC to measure the thermodynamic parameters of this binding reaction. The *Mx*Kat solution was loaded in the cell, and the $NADP^+$ solution was titrated by injection into the cell. Figure 2B (upper panel) shows substantial heat released by the titration of $NADP^+$ into *Mx*Kat; the power profile displayed an obvious heat peak, and a sigmoid-shaped curve of the enthalpy change during the titration process was observed (Fig. 2B, lower panel). This result confirmed that there was an exothermic reaction between $NADP^+$ and *Mx*Kat. Thus, the ITC experiments confirmed the interaction of $NADP^+$ with *Mx*Kat in terms of thermodynamics. The binding affinity can be quantified using the binding constant K_B, which was $3.43 \times 10^5\ M^{-1}$ (K_D [equilibrium dissociation constant], 2.92 μM) for $NADP^+$ binding to *Mx*Kat. Previous research demonstrated that the absolute metabolite concentration range of $NADP^+$ in *E. coli* is

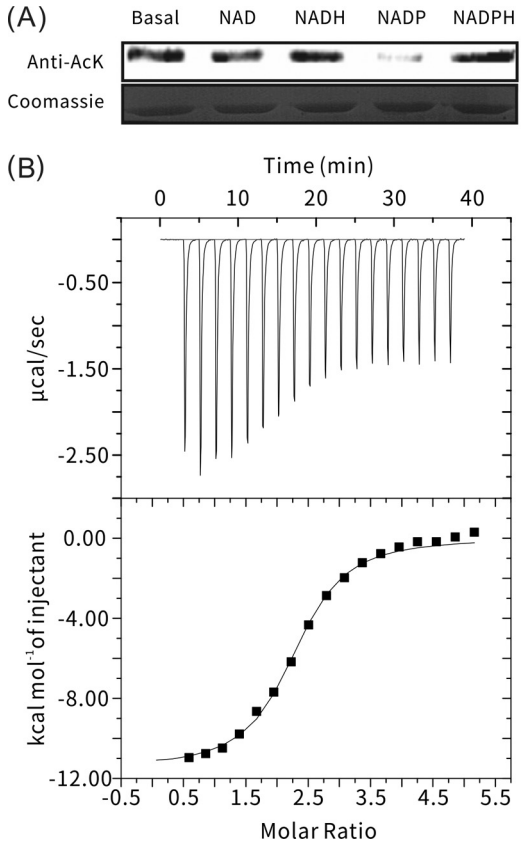

FIG 2 Screening of *Mx*Kat ligands. (A) Acetylation level was determined by Western blot analysis with acetyllysine antibodies after every coenzyme (NAD, NADH, $NADP^+$, and NADPH) bound with *Mx*Kat (upper panel). At the same time, another protein gel was stained with Coomassie brilliant blue (lower panel). (B) $NADP^+$ binding to *Mx*Kat was validated using ITC. Purified *Mx*Kat was dissolved in 1 M PBS (pH 7.4) to a final concentration of up to 38 μM. Meanwhile, $NADP^+$ was dissolved in PBS to 1 mM and used to inject for titration. Deionized water was used as a blank control.

0.14 to 31.1 μM (49). Therefore, the ITC data combined with Western blot results indicate that $NADP^+$ can bind to *Mx*Kat at physiologic concentrations and may negatively regulate the function of *Mx*Kat to acetylate *Mx*Acs.

***Mx*Kat may function as an $NADP^+$-regulated protein acetyltransferase.** *In silico* analysis combined with the Western blotting assay described above demonstrated that *Mx*Kat is a protein lysine acetyltransferase that can acetylate *Mx*Acs. As shown in Fig. 3A, the acetylation of *Mx*Acs was observed during incubation with *Mx*Kat and acetyl-CoA, and acetylation significantly decreased in the presence of $NADP^+$. The $NADP^+$-binding domain fused to the acetyltransferase domain in *Mx*Kat. The observed decrease in the acetylation level of *Mx*Acs in the presence of $NADP^+$ indicates that the $NADP^+$ domain may regulate the activity of the GNAT domain and that *Mx*Kat can function as an $NADP^+$-regulated protein acetyltransferase. In support of this hypothesis, in the presence of $NADP^+$, *Mx*Kat activity exhibited a ligand concentration-dependent decrease in protein acetylation (Fig. 3B).

To further test whether $NADP^+$ can regulate the acetylation activity of *Mx*Kat, we investigated the *Mx*Kat enzyme activity in the presence or absence of $NADP^+$. The acetylation reaction of *Mx*Kat was monitored by a coupled enzymatic assay, in which the amount of CoA liberated following acetylation is measured according to the formation of reduced NADH from NAD^+ by pyruvate dehydrogenase (38, 39). In the presence of $NADP^+$, the enzyme activity of *Mx*Kat was significantly attenuated compared to that in the absence of $NADP^+$ (Fig. 3C), which indicates that $NADP^+$ negatively modulated *Mx*Kat. Furthermore, we were also interested in the effect of $NADP^+$ binding on the enzyme activity of *Mx*Acs upon *Mx*Kat acetylation. Therefore, we used a coupled enzymatic assay to continuously monitor the catalytic reaction of the acetylated *Mx*Acs. As shown in Fig. 3D, in the presence of $NADP^+$, low *Mx*Kat activity resulted in a low acetylation level of *Mx*Acs, revealing a higher level of enzyme activity of *Mx*Acs than that in the absence of $NADP^+$. Taken together, these results demonstrate that *Mx*Kat acetylated *Mx*Acs and that the acetylation was mediated by $NADP^+$.

A previous study demonstrated that bacterial acetyltransferases recognize a specific lysine site for protein acetylation, and an acetylation motif (PXXXXGK) was proposed in AMP-forming Acs (9). In the present study, we confirmed that GNAT acetyltransferases can recognize this motif and acetylate its last lysine residue, such as Lys617 of *Mt*Acs from *M. tuberculosis*, Lys610 of *Sl*Acs from *Streptomyces lividans*, Lys606 of *Rp*Acs from *Rhodopseudomonas palustris*, Lys609 of *Ec*Acs from *E. coli*, and Lys609 of *Se*Acs from *S. enterica* (Fig. 4A).

To determine the specific site(s) used for acetylation in *Mx*Acs, *in vitro*-acetylated *Mx*Acs was separated by electrophoresis, and the band corresponding to *Mx*Acs was analyzed by MS. LC-MS confirmed that a peptide with sequence SGKIMR (419.2 Da) contained the major acetylated lysine residue (Lys622) (Fig. 4B) in the protein, which corresponds to the last lysine residue of the PXXXXGK motif.

To further validate the function of Lys622 in the acetylation of *Mx*Acs, we established substitution mutations at the Lys622 position to generate the K622Q variant of *Mx*Acs. Glutamine lacks a positive charge and therefore serves as a structural mimic for acetyllysine (12). $MxAcs^{K622Q}$ and $MxAcs^{WT}$ were incubated with the *Mx*Kat enzyme and acetyl-CoA. Western blotting was conducted to detect the acetylation level of $MxAcs^{WT}$ and $MxAcs^{K622Q}$ with an anti-acetyllysine antibody. As shown in Fig. 4C, the acetylation of $MxAcs^{WT}$ only was observed. No acetylation of $MxAcs^{K622Q}$ was observed, which indicated that *Mx*Kat modified the conserved lysine residue, Lys622, of the major active site in *Mx*Acs.

Identification of residues in the $NADP^+$-binding domain associated with $NADP^+$ binding. The NAD(P)-binding domain is widely present in the short-chain dehydrogenase/reductase (SDR) family, whose members contain a single domain with a structurally conserved Rossmann fold, an NAD(P)(H)-binding region, and a structurally diverse C-terminal region. The Rossmann fold is a common structural motif found in proteins that bind to nucleotides, especially the cofactor NAD(P). The structure with two repeats is composed of six parallel β-strands linked to two pairs of α-helices in the topological order β-α-β-α-β. The Rossmann fold is one of the three most highly represented folds in the Protein Data Bank (PDB), and it often can be identified by the short consensus amino acid sequence motif $GX_{1-2}GXXG$ (50). The $NADP^+$-binding domain of *Mx*Kat was analyzed using the CDD (36) (http://www.ncbi.nlm.nih.gov/Structure/cdd/wrpsb.cgi). As shown in Fig. 5A, *Mx*Kat has only one motif similar to the $GX_{1-2}GXXG$ motif and two Gly residues distributed at the 9 and 11 positions. In the three-dimensional protein model, we found

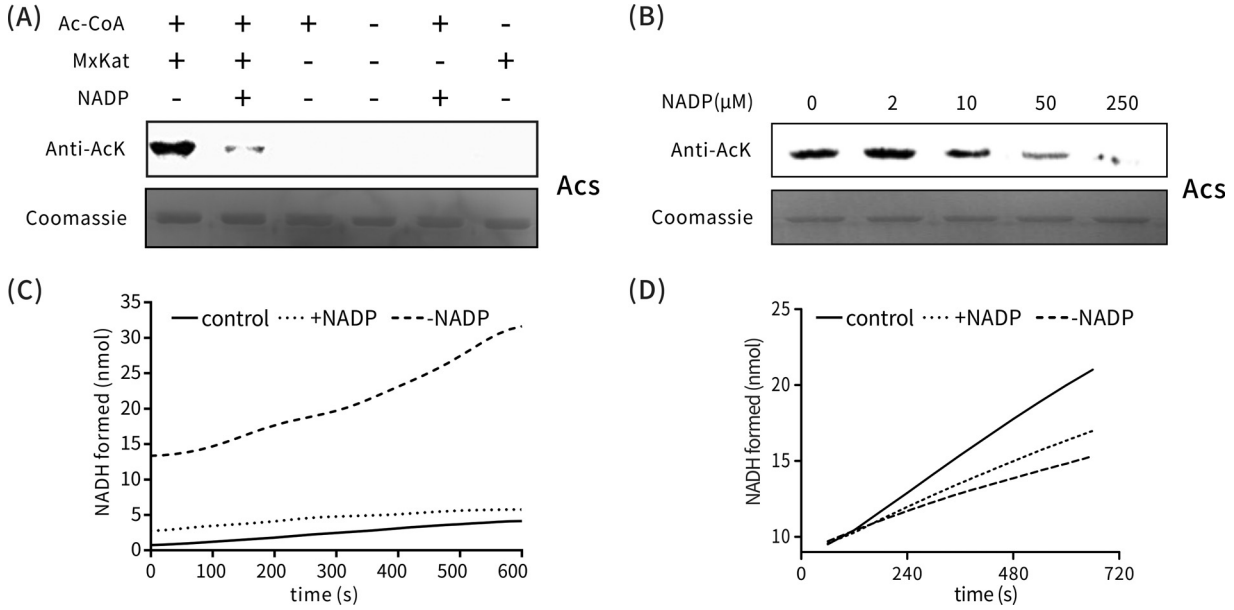

FIG 3 Regulation of *Mx*Kat activity for protein acetylation by $NADP^+$. (A) Acetylation of *Mx*Acs (Mxan_2570) by *Mx*Kat. *Mx*Acs (10 μg) was incubated alone or in the presence of *Mx*Kat (0.2 μM), acetyl-CoA (60 μM), and $NADP^+$ (2 μM) in a 100-μl volume at 37°C for 60 min, followed by SDS-PAGE analysis. The acetylation level was determined by Western blot analysis with acetyllysine antibodies (upper panel). At the same time, another protein electrophoresis gel was stained with Coomassie brilliant blue (lower panel). (B) Acetylation levels of *Mx*Acs were measured using a Western blot assay. With fixed concentrations of *Mx*Acs (1.5 μM), *Mx*Kat (0.2 μM), and acetyl-CoA (60 μM), various concentrations of $NADP^+$ were added to the reaction system. The reaction lasted 60 min at 37°C and was followed by SDS-PAGE analysis. (C) Acetyltransferase activity of *Mx*Kat was measured using a coupled enzymatic assay. The initial rate of formation of NADH is shown in the presence or absence of $NADP^+$. The control represents an assay in which PBS buffer was used instead of *Mx*Kat. (D) Enzymatic activity of *Mx*Acs. In the presence of $NADP^+$, the acetylation of *Mx*Acs was attenuated; thus, the enzyme activity of *Mx*Acs was higher in the presence than in the absence of $NADP^+$. The control represents an assay in which PBS buffer was used in place of *Mx*Kat.

that the G9 residue is likely located at the end of the β-sheet, whereas the G11 residue may be located between the α-helix and β-sheet (see Fig. S3 in the supplemental material). To determine the roles of these residues in $NADP^+$ binding, site-directed mutagenesis was performed to convert the Gly to Ala at residues 9 and 11. The acetylation activities of the wild-type and mutant proteins in the presence of $NADP^+$ were also determined using a coupled acetyltransferase enzyme assay and Western blot analysis.

When Gly9 was mutated to Ala, the enzyme activity of *Mx*Kat^{G9A} was still negatively regulated by $NADP^+$, as observed for wild-type *Mx*Kat (Fig. 5B). However, when Gly11 was mutated to Ala, no change in the activity of acetyltransferase was observed in the presence or absence of $NADP^+$, which indicated that *Mx*Kat^{G11A} was no longer modulated by $NADP^+$ (Fig. 5C). The CD spectra (Fig. 5D) of *Mx*Kat and the G11A mutant were nearly identical in the far-UV region (200 to 260 nm), in which the signals arose from the *Mx*Kat chain structure. These data showed that the G11A mutation likely did not perturb the structure of the NAD^+-binding domain of *Mx*Kat. Taken together, these results indicated that Gly11 of *Mx*Kat is involved in the interaction with $NADP^+$ and is part of the active site for the $NADP^+$-mediated regulation of *Mx*Kat.

DISCUSSION

Many deacetylases require coenzyme NAD^+ to effectively remove the acetyl group from an acetylated protein. Our study further uncovered a new biochemical mechanism whereby the coenzyme $NADP^+$ negatively regulates an acetyltransferase to reduce the acetylation level of specific intracellular proteins. These findings help deepen our understanding of the biochemical mechanism of how acetylation controls the activity/function of a metabolic enzyme by inducing a change in the $NADP^+$ coenzyme.

$NADP^+$ synthesis proceeds through two major mechanisms: $NADP^+$ can be generated *de novo* from NAD^+ through the action of NAD^+ kinases (NADKs), or $NADP^+$ might be formed from NADPH via the action of multiple NADPH-dependent enzymes, such as glutathione reductase (51). Although $NADP^+$ is known to play several important regulatory roles, its regulatory mechanism with respect to acetylation has received little attention thus far. The major known biological function of $NADP^+$ is as a precursor for NADPH formation (52). Furthermore, the mechanism and subcellular localization of $NADP^+$ and NADPH generation appear to critically influence the physiological state of a cell and, therefore, cell survival. Furthermore, NADKs have been shown to regulate the formation of $NADP^+$ from NAD^+, which can be inhibited by NADPH (53). In this study, we found that NADPH did not affect the ability of *Mx*Kat to acetylate *Mx*Acs (Fig. 2A), and the $NADP^+$ modulation of *Mx*Kat was concentration dependent (Fig. 3B). Therefore, the homeostasis of $NADP^+$ plays a crucial role in regulating *Mx*Kat, similar to the balance of NAD^+ and NADH in mediating deacetylases.

Another study showed that the activities of protein acetyltransferases and deacetylases are carefully regulated in response to a change in the intracellular signals that control the acetylation of specific proteins (such as the level of acetyl-CoA or NAD^+), which in turn affects the metabolic network (11). Acetyl-CoA and NAD^+ are key indicators of cellular energy status, and protein lysine acetylation serves as a link that connects cellular energy levels to protein acetylation/deacetylation activity. In mycobacteria, cAMP directly activates *Ms*Kat and *Mt*Kat by binding to the cyclic

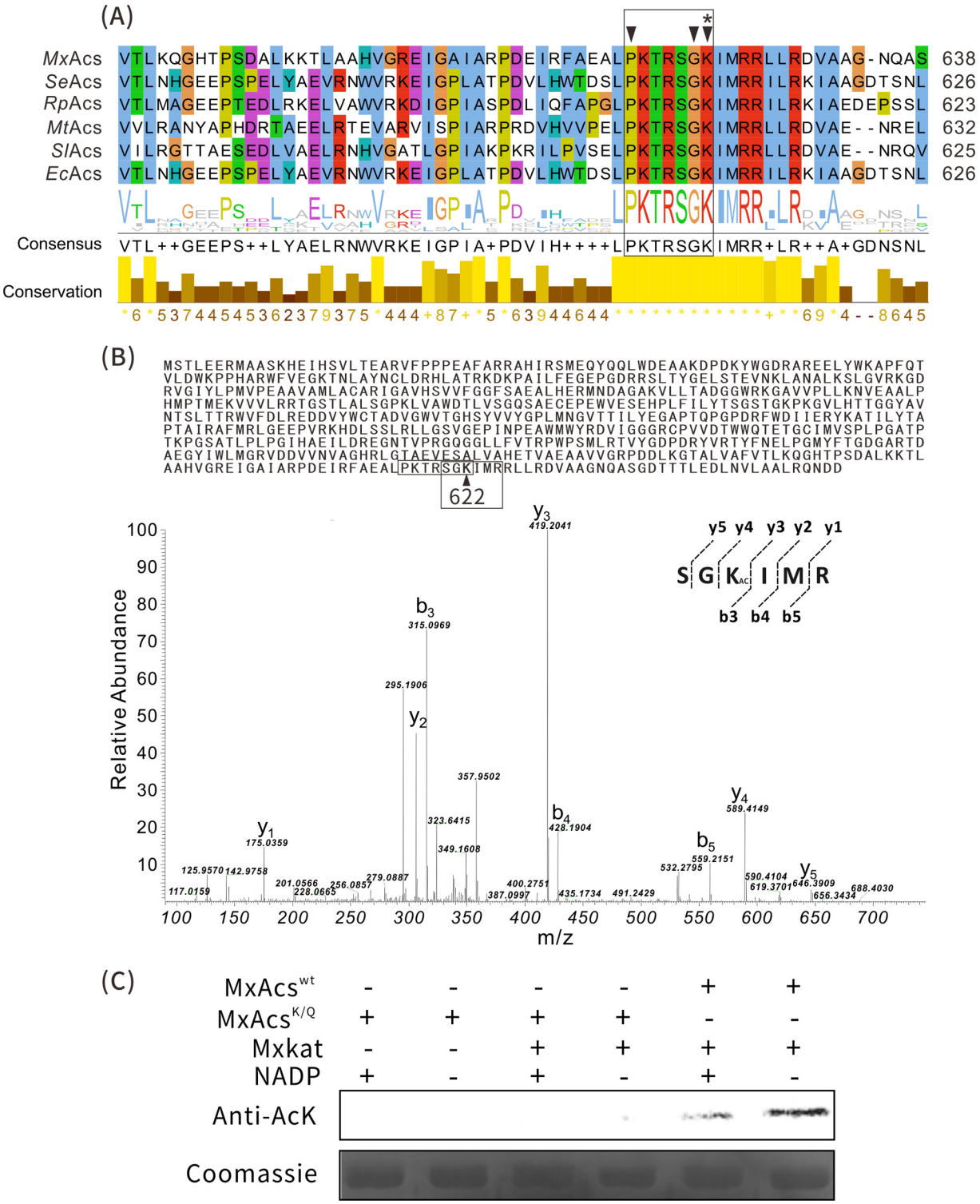

FIG 4 Lys622 residue of *Mx*Acs is acetylated by *Mx*Kat. (A) Sequence alignment of acetyl-CoA synthetases (Acs); a conserved PKXXXXK motif (boxed region) in Acs was found in *Mx*Acs (Mxan_2570). Key amino acids and the acetylated site are marked with arrowheads and an asterisk, respectively. (B) LC-MS/MS spectrum of a tryptic peptide with a mass/charge ratio (*m/z*) of 419.2 obtained from acetylated *Mx*Acs. This spectrum matched that of the peptide (boxed sequence) in *Mx*Acs (inset shows the sequence of the purified protein), with a mass shift in the b3 and y4 ions corresponding to acetylation at the lysine residue (arrowhead at position 622). (C) Western blot analysis of *Mx*Acs upon acetylation of *Mx*Kat. Wild-type *Mx*Acs or the *Mx*Acs^{K622Q} mutant was incubated with various components at 37°C for 60 min, followed by SDS-PAGE analysis. The reaction was performed in the presence and absence of NADP$^+$.

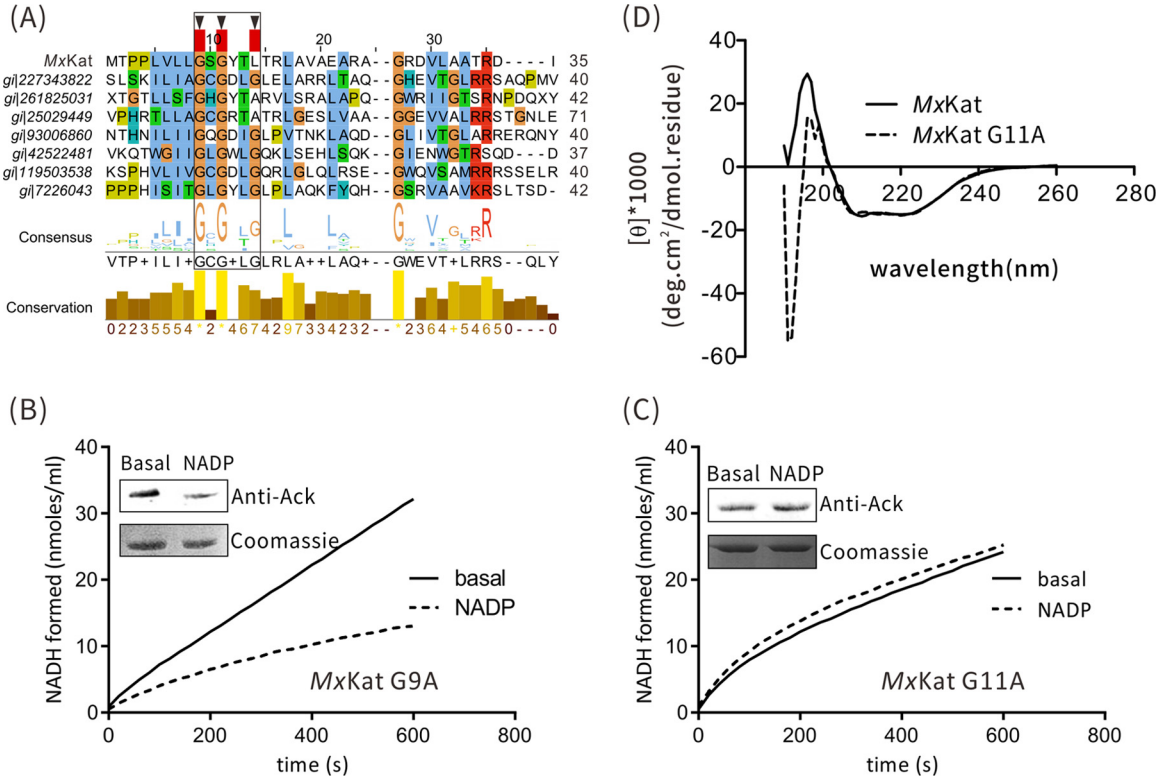

FIG 5 NADP$^+$-binding sites of *Mx*Kat. (A) Binding motif of the NAD(P) domain of *Mx*Kat. (B and C) Initial rates of NADH formation and Western blot analysis are shown for the *Mx*Kat mutants (the G9A and G11A mutants, respectively). The basal level represents the enzyme activity of wild-type *Mx*KAT. (Inset) MxAcs was acetylated by *Mx*Kat G9A and *Mx*Kat G11A in the presence or absence of NADP$^+$. The acetylation level was determined by Western blotting with acetyllysine antibodies (upper panel). At the same time, another protein gel was stained with Coomassie brilliant blue (lower panel). (D) Circular dichroism assays showed that the G11A mutant does not perturb the NADP$^+$-binding domain structure of *Mx*Kat.

nucleotide-binding (CNB) domain of two protein acetyltransferases, indicating that the levels of protein acetylation can also be modulated in response to changes in intracellular cAMP levels (54). This work demonstrated that the NADP$^+$ domain is linked to GNAT acetyltransferase, which confirms NADP$^+$-induced regulation of this enzyme. Therefore, protein acetyltransferases with an NADP$^+$-GNAT domain organization might be a novel mechanism in response to the homeostasis of intracellular coenzymes.

The coenzyme NADP$^+$ can be transformed to NADPH to maintain the intracellular redox potential by glucose-6-phosphate dehydrogenase (G6PD), 6-glyconate phosphate dehydrogenase (6GPD), NADP$^+$-dependent isocitrate dehydrogenases (IDPs), and NADP$^+$-dependent malic enzymes (MEPs), which are involved in glycolysis, gluconeogenesis, glycogen metabolism, and the TCA cycle. Moreover, these sugar metabolism-related enzymes have been shown to be regulated by lysine acetylation, which results in a reduction in enzyme activity (5–7). Low acetylation levels of the associated enzymes result in a high intracellular NADP$^+$-to-NADPH ratio. Since NADP$^+$ was found to modulate the protein acetyltransferase *Mx*Kat, it is possible that a high NADP$^+$-to-NADPH ratio would influence the NADP$^+$-mediated acetylation of some proteins, including enzymes involved in the conversion between NADP$^+$ and NADPH. Future work will focus on the identification of all substrates of the *Mx*Kat enzyme and aim to reveal the complete landscape of NADP$^+$-mediated acetylation.

To our knowledge, this study is the first to demonstrate the allosteric regulation of a protein acetyltransferase by NADP$^+$, which indicates that the intracellular acetylation levels of proteins might be modulated in response to changes in the NADP$^+$-to-NADPH ratio. This finding might provide the basis for uncovering the molecular mechanism underlying the homeostasis of protein acetylation/deacetylation in response to changes in intracellular signals.

ACKNOWLEDGMENT

We thank Yue-zhong Li of Shandong University for kindly providing the *M. xanthus* DK1622 strain.

FUNDING INFORMATION

Chinese Ministry of Education provided funding to Bang-Ce Ye under grant number SRFDP 20120074110009. National Natural Science Foundation of China (NSFC) provided funding to Bang-Ce Ye under grant number 21276079.

This work was also supported by grants from the National Key Technologies R&D Programs (2014AA021502), Fundamental Research Funds for the Central Universities, and the Shanghai Natural Science Foundation (14ZR1409600).

REFERENCES

1. **Hu LI, Lima BP, Wolfe AJ.** 2010. Bacterial protein acetylation: the dawning of a new age. Mol Microbiol **77:**15–21. http://dx.doi.org/10.1111/j.1365-2958.2010.07204.x.
2. **Kim GW, Yang XJ.** 2011. Comprehensive lysine acetylomes emerging from bacteria to humans. Trends Biochem Sci **36:**211–220. http://dx.doi.org/10.1016/j.tibs.2010.10.001.

3. **Hentchel KL, Escalante-Semerena JC.** 2015. Acylation of biomolecules in prokaryotes: a widespread strategy for the control of biological function and metabolic stress. Microbiol Mol Biol Rev **79:**321–346. http://dx.doi.org/10.1128/MMBR.00020-15.
4. **Thao S, Escalante-Semerena JC.** 2011. Control of protein function by reversible N^{ε}-lysine acetylation in bacteria. Curr Opin Microbiol **14:**200–204. http://dx.doi.org/10.1016/j.mib.2010.12.013.
5. **Weinert BT, Iesmantavicius V, Wagner SA, Schölz C, Gummesson B, Beli P, Nyström T, Choudhary C.** 2013. Acetyl-phosphate is a critical determinant of lysine acetylation in *E. coli*. Mol Cell **51:**265–272. http://dx.doi.org/10.1016/j.molcel.2013.06.003.
6. **Zhang K, Tian S, Fan E.** 2013. Protein lysine acetylation analysis: current MS-based proteomic technologies. Analyst **138:**1628–1636. http://dx.doi.org/10.1039/c3an36837h.
7. **Kuhn ML, Zemaitaitis B, Hu LI, Sahu A, Sorensen D, Minasov G, Lima BP, Scholle M, Mrksich M, Anderson WF, Gibson BW, Schilling B, Wolfe AJ.** 2014. Structural, kinetic and proteomic characterization of acetyl phosphate-dependent bacterial protein acetylation. PLoS One **9:**e94816. http://dx.doi.org/10.1371/journal.pone.0094816.
8. **Schilling B, Christensen D, Davis R, Sahu AK, Hu LI, Walker-Peddakotla A, Sorensen DJ, Zemaitaitis B, Gibson BW, Wolfe AJ.** 2015. Protein acetylation dynamics in response to carbon overflow in *Escherichia coli*. Mol Microbiol **98:**847–863. http://dx.doi.org/10.1111/mmi.13161.
9. **Starai VJ, Celic I, Cole RN, Boeke JD, Escalante-Semerena JC.** 2002. Sir2-dependent activation of acetyl-CoA synthetase by deacetylation of active lysine. Science **298:**2390–2392. http://dx.doi.org/10.1126/science.1077650.
10. **You D, Yao LL, Huang D, Escalante-Semerena JC, Ye B-C.** 2014. Acetyl coenzyme A synthetase is acetylated on multiple lysine residues by a protein acetyltransferase with a single Gcn5-type *N*-acetyltransferase (GNAT) domain in *Saccharopolyspora erythraea*. J Bacteriol **196:**3169–3178. http://dx.doi.org/10.1128/JB.01961-14.
11. **Xu J-Y, You D, Leng P-Q, Ye B-C.** 2014. Allosteric regulation of a protein acetyltransferase in *Micromonospora aurantiaca* by the amino acids cysteine and arginine. J Biol Chem **289:**27034–27045. http://dx.doi.org/10.1074/jbc.M114.579078.
12. **Tucker AC, Escalante-Semerena JC.** 2013. Acetoacetyl-CoA synthetase activity is controlled by a protein acetyltransferase with unique domain organization in *Streptomyces lividans*. Mol Microbiol **87:**152–167. http://dx.doi.org/10.1111/mmi.12088.
13. **Wu X, Vellaichamy A, Wang D, Zamdborg L, Kelleher NL, Huber SC, Zhao Y.** 2013. Differential lysine acetylation profiles of *Erwinia amylovora* strains revealed by proteomics. J Proteomics **79:**60–71. http://dx.doi.org/10.1016/j.jprot.2012.12.001.
14. **Okanishi H, Kim K, Masui R, Kuramitsu S.** 2013. Acetylome with structural mapping reveals the significance of lysine acetylation in *Thermus thermophilus*. J Proteome Res **12:**3952–3968. http://dx.doi.org/10.1021/pr400245k.
15. **Lee DW, Kim D, Lee YJ, Kim JA, Choi JY, Kang S, Pan JG.** 2013. Proteomic analysis of acetylation in thermophilic *Geobacillus kaustophilus*. Proteomics **13:**2278–2282. http://dx.doi.org/10.1002/pmic.201200072.
16. **Crosby HA, Pelletier DA, Hurst GB, Escalante-Semerena JC.** 2012. System-wide studies of *N*-lysine acetylation in *Rhodopseudomonas palustris* reveal substrate specificity of protein acetyltransferases. J Biol Chem **287:**15590–15601. http://dx.doi.org/10.1074/jbc.M112.352104.
17. **Ramponi G, Manao G, Camici G.** 1975. Nonenzymatic acetylation of histones with acetyl phosphate and acetyl adenylate. Biochemistry **14:**2681–2685. http://dx.doi.org/10.1021/bi00683a018.
18. **AbouElfetouh A, Kuhn ML, Hu LI, Scholle MD, Sorensen DJ, Sahu AK, Becher D, Antelmann H, Mrksich M, Anderson WF, Gibson BW, Schilling B, Wolfe AJ.** 2015. The *E. coli* sirtuin CobB shows no preference for enzymatic and nonenzymatic lysine acetylation substrate sites. Microbiologyopen **4:**66–83. http://dx.doi.org/10.1002/mbo3.223.
19. **Shaw KJ, Rather PN, Hare RS, Miller GH.** 1993. Molecular genetics of aminoglycoside resistance genes and familial relationships of the aminoglycoside-modifying enzymes. Microbiol Rev **57:**138–163.
20. **Vetting MW, S de Carvalho LP, Yu M, Hegde SS, Magnet S, Roderick SL, Blanchard JS.** 2005. Structure and functions of the GNAT superfamily of acetyltransferases. Arch Biochem Biophys **433:**212–226. http://dx.doi.org/10.1016/j.abb.2004.09.003.
21. **Ikeuchi Y, Kitahara K, Suzuki T.** 2008. The RNA acetyltransferase driven by ATP hydrolysis synthesizes *N*4-acetylcytidine of tRNA anticodon. EMBO J **27:**2194–2203. http://dx.doi.org/10.1038/emboj.2008.154.
22. **Spange S, Wagner T, Heinzel T, Kramer OH.** 2009. Acetylation of non-histone proteins modulates cellular signalling at multiple levels. Int J Biochem Cell Biol **41:**185–198. http://dx.doi.org/10.1016/j.biocel.2008.08.027.
23. **Thao S, Chen CS, Zhu H, Escalante-Semerena JC.** 2010. N^{ε}-Lysine acetylation of a bacterial transcription factor inhibits its DNA-binding activity. PLoS One **5:**e15123. http://dx.doi.org/10.1371/journal.pone.0015123.
24. **Grundy FJ, Turinsky AJ, Henkin TM.** 1994. Catabolite regulation of *Bacillus subtilis* acetate and acetoin utilization genes by CcpA. J Bacteriol **176:**4527–4533.
25. **Castaño-Cerezo S, Bernal V, Blanco-Catala J, Iborra JL, Canovas M.** 2011. cAMP-CRP co-ordinates the expression of the protein acetylation pathway with central metabolism in *Escherichia coli*. Mol Microbiol **82:**1110–1128. http://dx.doi.org/10.1111/j.1365-2958.2011.07873.x.
26. **Hentchel KL, Thao S, Intile PJ, Escalante-Semerena JC.** 2015. Deciphering the regulatory circuitry that controls reversible lysine acetylation in *Salmonella enterica*. mBio **6**(4):e00891-15. http://dx.doi.org/10.1128/mBio.00891-15.
27. **Nambi S, Basu N, Visweswariah SS.** 2010. cAMP-regulated protein lysine acetylases in mycobacteria. J Biol Chem **285:**24313–24323. http://dx.doi.org/10.1074/jbc.M110.118398.
28. **Lee HJ, Lang PT, Fortune SM, Sassetti CM, Alber T.** 2012. Cyclic AMP regulation of protein lysine acetylation in *Mycobacterium tuberculosis*. Nat Struct Mol Biol **19:**811–818. http://dx.doi.org/10.1038/nsmb.2318.
29. **Nambi S, Badireddy S, Visweswariah SS, Anand GS.** 2012. Cyclic AMP-induced conformational changes in mycobacterial protein acetyltransferases. J Biol Chem **287:**18115–18129. http://dx.doi.org/10.1074/jbc.M111.328112.
30. **Podobnik M, Siddiqui N, Rebolj K, Nambi S, Merzel F, Visweswariah SS.** 2014. Allostery and conformational dynamics in cAMP-binding acyltransferases. J Biol Chem **289:**16588–16600. http://dx.doi.org/10.1074/jbc.M114.560086.
31. **Wang YP, Zhou LS, Zhao YZ, Wang SW, Chen LL, Liu LX, Ling ZQ, Hu FJ, Sun YP, Zhang JY, Yang C, Yang Y, Xiong Y, Guan KL, Ye D.** 2014. Regulation of G6PD acetylation by KAT9/SIRT2 modulates NADPH homeostasis and cell survival during oxidative stress. EMBO J **33:**1304–1320.
32. **Kim SY, Lee SM, Tak JK, Choi KS, Kwon TK, Park JW.** 2007. Regulation of singlet oxygen-induced apoptosis by cytosolic $NADP^{+}$-dependent isocitrate dehydrogenase. Mol Cell Biochem **302:**27–34. http://dx.doi.org/10.1007/s11010-007-9421-x.
33. **Mikulik K, Felsberg J, Kudrnáčová E, Bezoušková S, Setinová D, Stodůlková E, Zídková J, Zídek V.** 2012. CobB1 deacetylase activity in *Streptomyces coelicolor*. Biochem Cell Biol **90:**179–187. http://dx.doi.org/10.1139/o11-086.
34. **Denu JM.** 2005. The Sir2 family of protein deacetylases. Curr Opin Chem Biol **9:**431–440. http://dx.doi.org/10.1016/j.cbpa.2005.08.010.
35. **Zhao X, Allison D, Condon B, Zhang FY, Gheyi T, Zhang AP, Ashok S, Russell M, MacEwan I, Qian YW, Jamison JA, Luz JG.** 2013. The 2.5 Å crystal structure of the SIRT1 catalytic domain bound to nicotinamide adenine dinucleotide (NAD+) and an indole (EX527 analogue) reveals a novel mechanism of histone deacetylase inhibition. J Med Chem **56:**963–969. http://dx.doi.org/10.1021/jm301431y.
36. **Marchler-Bauer A, Zheng C, Chitsaz F, Derbyshire MK, Geer LY, Geer RC, Gonzales NR, Gwadz M, Hurwitz DI, Lanczycki CJ, Lu F, Lu S, Marchler GH, Song JS, Thanki N, Yamashita RA, Zhang D, Bryant SH.** 2013. CDD: conserved domains and protein three-dimensional structure. Nucleic Acids Res **41:**D348–D352. http://dx.doi.org/10.1093/nar/gks1243.
37. **Tamura K, Stecher G, Peterson D, Filipski A, Kumar S.** 2013. MEGA6: Molecular Evolutionary Genetics Analysis version 6.0. Mol Biol Evol **30:**2725–2729. http://dx.doi.org/10.1093/molbev/mst197.
38. **Berndsen CE, Denu JM.** 2005. Assays for mechanistic investigations of protein/histone acetyltransferases. Methods **36:**321–331. http://dx.doi.org/10.1016/j.ymeth.2005.03.002.
39. **Kim Y, Tanner KG, Denu JM.** 2000. A continuous, nonradioactive assay for histone acetyltransferases. Anal Biochem **280:**308–314. http://dx.doi.org/10.1006/abio.2000.4546.
40. **Zhang J, Sprung R, Pei J, Tan X, Kim S, Zhu H, Liu CF, Grishin NV, Zhao Y.** 2009. Lysine acetylation is a highly abundant and evolution-

arily conserved modification in *Escherichia coli*. Mol Cell Proteomics **8:**215–225.
41. **Finn RD, Bateman A, Clements J, Coggill P, Eberhardt RY, Eddy SR, Heger A, Hetherington K, Holm L, Mistry J, Sonnhammer EL, Tate J, Punta M.** 2014. Pfam: the protein families database. Nucleic Acids Res **42:**D222–D230. http://dx.doi.org/10.1093/nar/gkt1223.
42. **Schuetz A, Bernstein G, Dong A, Antoshenko T, Wu H, Loppnau P, Bochkarev A, Plotnikov AN.** 2007. Crystal structure of a binary complex between human GCN5 histone acetyltransferase domain and acetyl coenzyme A. Proteins **68:**403–407.
43. **Trievel RC, Rojas JR, Sterner DE, Venkataramani RN, Wang L, Zhou J, Allis CD, Berger SL, Marmorstein R.** 1999. Crystal structure and mechanism of histone acetylation of the yeast GCN5 transcriptional coactivator. Proc Natl Acad Sci U S A **96:**8931–8936. http://dx.doi.org/10.1073/pnas.96.16.8931.
44. **Poux AN, Cebrat M, Kim CM, Cole PA, Marmorstein R.** 2002. Structure of the GCN5 histone acetyltransferase bound to a bisubstrate inhibitor. Proc Natl Acad Sci U S A **99:**14065–14070. http://dx.doi.org/10.1073/pnas.222373899.
45. **Neuwald AF, Landsman D.** 1997. GCN5-related histone *N*-acetyltransferases belong to a diverse superfamily that includes the yeast SPT10 protein. Trends Biochem Sci **22:**154–155. http://dx.doi.org/10.1016/S0968-0004(97)01034-7.
46. **Biasini M, Bienert S, Waterhouse A, Arnold K, Studer G, Schmidt T, Kiefer F, Cassarino TG, Bertoni M, Bordoli L, Schwede T.** 2014. SWISS-MODEL: modelling protein tertiary and quaternary structure using evolutionary information. Nucleic Acids Res **42:**W252–W258. http://dx.doi.org/10.1093/nar/gku340.
47. **Starai VJ, Escalante-Semerena JC.** 2004. Identification of the protein acetyltransferase (Pat) enzyme that acetylates acetyl-CoA synthetase in *Salmonella enterica*. J Mol Biol **340:**1005–1012. http://dx.doi.org/10.1016/j.jmb.2004.05.010.
48. **Xu H, Hegde SS, Blanchard JS.** 2011. Reversible acetylation and inactivation of *Mycobacterium tuberculosis* acetyl-CoA synthetase is dependent on cAMP. Biochemistry **50:**5883–5892. http://dx.doi.org/10.1021/bi200156t.
49. **Bennett BD, Kimball EH, Gao M, Osterhout R, Van Dien SJ, Rabinowitz JD.** 2009. Absolute metabolite concentrations and implied enzyme active site occupancy in *Escherichia coli*. Nat Chem Biol **5:**593–599. http://dx.doi.org/10.1038/nchembio.186.
50. **Kleiger G, Eisenberg D.** 2002. GXXXG and GXXXA motifs stabilize FAD and NAD(P)-binding Rossmann folds through C(alpha)-H. . . O hydrogen bonds and van der Waals interactions. J Mol Biol **323:**69–76.
51. **Pollak N, Dölle C, Ziegler M.** 2007. The power to reduce: pyridine nucleotides—small molecules with a multitude of functions. Biochem J **402:**205–218. http://dx.doi.org/10.1042/BJ20061638.
52. **Ying W.** 2008. NAD^+/NADH and $NADP^+$/NADPH in cellular functions and cell death: regulation and biological consequences. Antioxid Redox Signal **10:**179–206. http://dx.doi.org/10.1089/ars.2007.1672.
53. **Zerez CR, Moul DE, Gomez EG, Lopez VM, Andreoli AJ.** 1987. Negative modulation of *Escherichia coli* NAD kinase by NADPH and NADH. J Bacteriol **169:**184–188.
54. **Nambi S, Gupta K, Bhattacharyya M, Ramakrishnan P, Ravikumar V, Siddiqui N, Thomas AT, Visweswariah SS.** 2013. Cyclic AMP-dependent protein lysine acylation in mycobacteria regulates fatty acid and propionate metabolism. J Biol Chem **288:**14114–14124. http://dx.doi.org/10.1074/jbc.M113.463992.